Desalination and Water Treatment
www.deswater.com

doi: 10.1080/19443994.2015.1017741

57 (2016) 7322–7333
April

Taylor & Francis
Taylor & Francis Group

Application of activated carbon derived from waste *Delonix regia* seed pods for the adsorption of acid dyes: kinetic and equilibrium studies

S.E. Subramani, D. Kumaresan, N. Thinakaran*

Environmental Research Lab, PG and Research Department of Chemistry, Alagappa Government Arts College, Karaikudi 630 003, Tamil Nadu, India, Tel. +91 9047383991; email: sesubramoni@gmail.com (S.E. Subramani), Tel. +91 8124373017; email: kumeresand@gmail.com (D. Kumaresan), Tel. +919488569001; email: thinakaran2k@yahoo.com (N. Thinakaran)

Received 12 July 2014; Accepted 1 February 2015

ABSTRACT

Activated carbon prepared from *Delonix regia* (DR) seed pod has been used as adsorbent for the removal of anionic dyes from aqueous solution. Three anionic textile dyes (C.I. Acid Blue 15, C.I. Acid Red 114, C.I. Acid Violet 17) and one dye mixture were used as model compounds. The capacity of DR to adsorb anionic dyes from aqueous dye solution was evaluated at different contact times, dosage, pH, and initial adsorbent concentration. Results show that the highest dye removal (>95%) was obtained at pH 2 for the adsorption of all the selected dyes. Four isotherms (Langmuir, Freundlich, Temkin, and Redlich–Peterson) were used to fit the equilibrium data. The adsorption equilibrium showed that the Langmuir equation represented best fit of the experimental data than others. The adsorption isotherm indicates that the adsorption capacities are 151.51, 113.63, and 129.87 mg dye per gram of DR for AR-114, AV-17, and AB-15 Acid dyes, respectively. In order to investigate the mechanism of adsorption and rate-controlling steps, pseudo-first-order, pseudo-second-order, intraparticle diffusion, and Elovich equations have been used to test the experimental data. The adsorption kinetics was found to follow pseudo-second-order kinetics with correlation coefficients greater than 0.99. It was found that at the higher initial acid dye concentration, intraparticle diffusion is becoming significant rate-controlling step.

Keywords: Acid dyes; Isotherms; Kinetics; *Delonix regia* seed pods

1. Introduction

Exploring effective and low-cost activated carbon may contribute to environmental sustainability and offer benefits for future commercial applications. Activated carbon is the most widely used adsorbent with great success because of its excellent adsorption capacity, but its use is limited due to its high cost. Furthermore, there are many problems associated with the regeneration of used activated carbon. In order to decrease the cost of treatment, some attempts have been made to find low-cost alternative adsorbents. As a result, many novel materials have been tested as adsorbents with two objectives: to replace activated carbon with inexpensive alternatives and to use various waste products as adsorbents [1]. Among the studied alternative materials are agricultural, forest, and animal byproducts such as peat, wheat bran, sawdust, tree barks, chitin, and others [2]. These include mango seed kernel [3], peanut hull [4], hazelnut shells [5], and Jute fiber [6]. A lot of agricultural waste

*Corresponding author.

byproducts have attracted good sources of raw materials to use as adsorbent whether in their raw or carbonized form. The frequently reported carbonization method in the literature is that of sulfuric acid treatment of agricultural waste byproducts such as jackfruit peel, corn stalk, apricot stone, and corncobs [2]. Several researchers have been studying the use of alternative materials that, although less efficient, involve lower costs. Natural materials that are available in large quantities may have potential as inexpensive sorbents. Due to their low cost, after these materials have been expended, they can be discarded without expensive regeneration. Moreover, certain type of agricultural material and its activation process is suitable for the maximum removal of certain type of dyes. Still, colored wastewater treatment needs new adsorbents that are economical, easily available, and effective.

Reverence of our mother's nature is exponentially diminishing due to human non-adherence to environmental laws in their thirst for technological advancement [7]. The complex structure of the synthetic dyes makes it very stable and difficult to degrade which leads to many environmental problems. Color removal from textile effluents has been the target in the last few years because of its potential toxicity to living organisms such as dysfunction of brain, kidney, liver, and central nervous system [8,9]. To protect the humans and the receiving ecosystem from contamination, it must be eliminated from before being released into the environment. The choice of *Delonix regia* (DR) seed pods is justified by the large availability of this material, in all parts of the world. Its major use today is as a combustible material, DR which is commonly called "Fire of the forest" or "May flower," so these solid wastes materials are converted into activated carbon with 18 N sulfuric acid and to study the removal of various acid dyes. The available literature indicates that due to a highly complex structure of the selected dyes and adsorbent, there have been no appropriate data so far that would enable modeling of the adsorption process The aim of the present work is to investigate the removal of some acid dyes; Acid Blue 15, Acid Red 114, Acid Violet 17, and a dye mixture AX from aqueous solutions by adsorption onto DR and to determine the adsorption characteristics of DR toward these dyes by conducting equilibrium and kinetic studies.

2. Experimental

2.1. Materials and methods

The adsorbate AB15, AR114, and AV17 were obtained from Sigma-Aldrich Corporation, Bangalore, India, and were used as such without any further purification. The stock solution was prepared by dissolving accurately weighed dye in distilled water to the concentration of 1,000 mg L^{-1}. The dye mixture is prepared by mixing equal concentration of dyes AR114 and AV17 at equal volume. The selected dyes characteristics and their chemical structures are shown in Table 1 and Fig. 1, respectively. All the other chemicals used were of analytical reagent grade and were purchased from Qualigens Fine Chemicals, Mumbai, India.

2.2. Preparation of activated adsorbents

DR seed pods were collected from local area of Karaikudi, Sivagangai district, Tamil Nadu, India. The seeds were removed from the seed pods and the empty pods were used for the preparation of adsorbents. The collected pods were dried in sunlight for several days to remove moisture content. Then the pods were cut into small pieces and soaked in 18 N sulfuric acid at 1:2 ratio (weight of raw material/volume of acid) for 36 h and activated at 120˚C in a muffle furnace (Gambaks Instruments, Chennai, India) for 12 h. The carbonized material obtained was washed several times with distilled water and dried at 120˚C for 6 h. The resultant material obtained was soaked in 5% sodium bicarbonate solution and allowed to stand overnight to remove the presence of any residual acid. The material was then thoroughly washed with distilled water and it was dried at 110˚C for 6 h. The resulting activated carbon material (DR) was dried in a hot air oven at 105˚C to remove the moisture, powdered, and sieved through a 0.25-mm sieve.

2.3. Batch adsorption experiments

Experiments with all the dyes and one mixture selected were performed to determine the adsorption equilibrium time. For each experimental run, 50-mL dye solution of known concentration, known pH, and a known amount of the adsorbent was placed in a 250-mL stoppered conical flask. The mixture was agitated in a temperature-controlled orbital shaker (Remi RIS 24^{+}) at a constant speed of 200 cycles per minute at 30 ± 1˚C. The adsorption isotherm experiment was carried out by agitating 50 mL of dye solutions of various concentrations. Samples were withdrawn at appropriate time intervals and the adsorbent was separated from dye solution by centrifugation (Remi) at 2,500 rpm for 5 min. The residual dye concentration was measured by collecting the supernatant and measuring the concentration using a UV–vis spectrophotometer (Systronics

Table 1
Characteristics of adsorbates

Parameters	C.I. Acid Red 114	C.I. Acid Blue 15	C.I. Acid Violet 17
Molecular formula	$C_{37}H_{28}N_4O_{10}S_3Na_2$	$C_{42}H_{46}N_3NaO_6S_2$	$C_{41}H_{44}N_3NaO_6S_2$
Purity (%)	80	90	90
Chromophore	Diazo	Triphenyl methane	Triphenyl methane
Molecular weight	830	775.96	761.93
λMAX (nm)	522	564	587
Appearance	Dark red powder	Violet powder	Dark blue powder

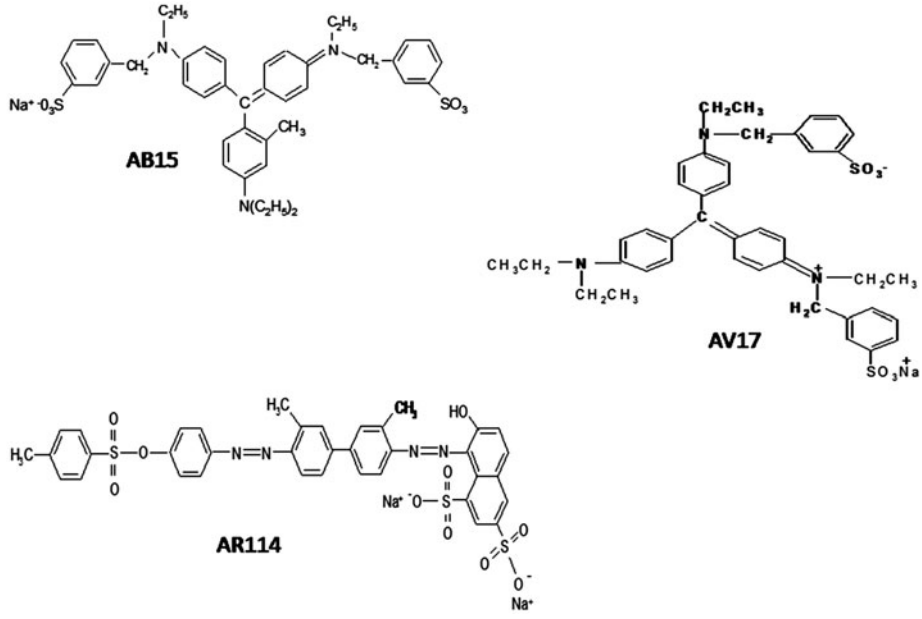

Fig. 1. Chemical structures of dyes (AR114, AV17, and AB15).

114) at an absorbance wavelength of 522 (AR114), 564 (AB15), and 587 (AV17) and 608 (AX) nm, respectively. The effect of pH on dye removal was studied over a pH range of 2–11 for all the adsorbates. The initial pH of the solution was adjusted by addition of dilute aqueous solutions of HCl or NaOH (0.1 M). The kinetic experiments were carried out using a known weight of adsorbent with 500 ml of the solution containing the dye in the concentration range of 60–100 mg L^{-1} in an overhead stirrer (Remi Lab Stirrer). At predetermined time intervals, portions of the mixture were withdrawn and then centrifuged. The residual dye concentration was then determined.

The percentage removal and amount adsorbed were calculated using the following relationships:

$$\text{Percentage removal} = \frac{C_i - C_t}{C_i} \times 100 \quad (1)$$

$$\text{Amount adsorbed } (q_e) = \frac{(C_i - C_t)V}{m} \quad (2)$$

where C_i and C_t are the initial and concentration at time t (mg L^{-1}) of dye, respectively, m is the weight (g) of adsorbent, and V is the volume of dye solution (L).

3. Results and discussion

3.1. Characterization of the adsorbent

To investigate the surface characteristics of DR FT-IR spectrum (Bruker Optik GmbH TENSOR 27) in the range of 450–4,000 cm^{-1} were studied. Fig. 2 shows the FT-IR spectrum of the adsorbent used in this study. Due to low-temperature carbonization (160°C) of the flame tree pods, the FT-IR spectra of the adsorbent reveal a number of absorption peaks, indicating that the adsorbent surface contains many functional

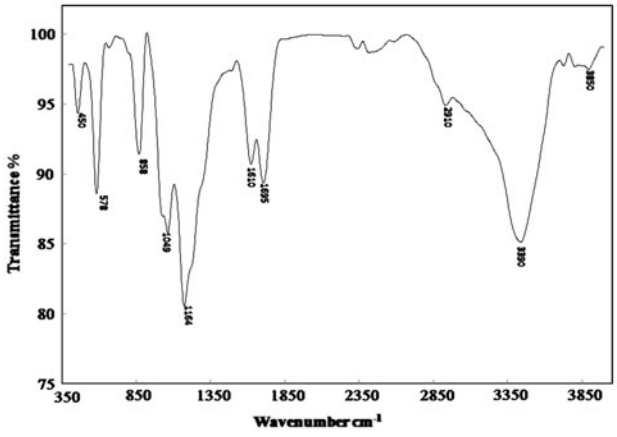

Fig. 2. FT-IR spectra of DR.

groups. The bands around 3,400 cm^{-1} are due to O–H stretching vibration of alcohols, phenols, and carboxylic acids as in pectin, cellulose, and lignin [10]. A band at 2,910 is due to the aliphatic CH stretching of methyl group and a sharp band around 1,695 and 1,610 is due to stretching vibrations of C=O and N–H groups, respectively. The peaks around 1,050 cm^{-1} are due to OCH_3 group which may be attributed to the lignin aromatic groups. Peaks around 580 cm^{-1} can be assigned to the bending modes of aromatic compounds [11]. The presence of these functional groups on the surface is likely to give considerable anion exchange capacity to the adsorbents [12].

The untreated DR seed pod powder has the surface area 6.38 $m^2 g^{-1}$ and also it has high-volatile matter (Table 2). From the surface area measurements and proximate and ultimate analysis, the untreated DR has poor adsorption characteristics compared to treated DR The surface area of the adsorbent DR (15.6 $m^2 g^{-1}$) was measured by N_2 adsorption at 77 K using Nova 4200e (Quantachrome Corp.). The particle morphology of the adsorbent DR was examined using HRSEM FEG (Quanta Microscope, Netherland) (SEM). The surface structure of DR was analyzed using SEM with a magnification of 5,000×. From Fig. 3, the surface morphology of the carbon obtained from the flame tree pods appears to have uneven surface with pores, where there is a good possibility for dye molecules to be trapped and adsorbed into these pores.

3.2. Effect of adsorbent dosage

The effect of adsorbent dosage was studied by varying the adsorbent dosage (0.5–4 g L^{-1}) on removal of all the selected acid dyes and its mixture by the adsorbent DR. Fig. 4 shows the plot between amount of dye adsorbed q_e against adsorbent concentration (g). From figure, it was observed that the amount of dye adsorbed gets varied with varying sorbent mass and it decreased with increase in adsorbent mass. The amount of dye adsorbed decreases from 113 to 29 for AV17, 100 to 25 for AR114, 130 to 29 for AB15, and 157 to 30 mg g^{-1} for AX an increase in adsorbent mass from 0.5 to 4 g L^{-1}. Whereas the percentage color removal increased from 42 to 99% with an increase in adsorbent mass from 0.5 to 0.4 g L^{-1}. Fig. 4 also revealed that the dye removal increased up to a certain limit and then it remains almost constant in all the cases. This was due to the availability of more adsorbent sites and high specific surfaces of the adsorbents [13]. The decrease in amount of dye adsorbed q_e (mg g^{-1}) with increasing adsorbent mass is due to the separation of the concentration gradient between solute concentration in the solution and the solute concentration in the surface of the adsorbent [14].

Table 2
Physicochemical characteristics of treated and untreated DR

Parameters	Treated DR	Untreated DR
Total surface area (BET) ($m^2 g^{-1}$)	15.6	6.38
Proximate analysis		
Moisture content (%)	0.71	12.2
Ash content (%)	2.5	14.3
Fixed carbon (%)	72	55
Volatile matter	6.21	18
Ultimate analysis		
Carbon (%)	64.46	42.36
Hydrogen (%)	5.22	10.23
Oxygen (%)	28.63	38.47
Nitrogen (%)	1.47	2.67
pH solution (10 mass%)	3.2	4.6
pH_{zpc}	3.9	6.4

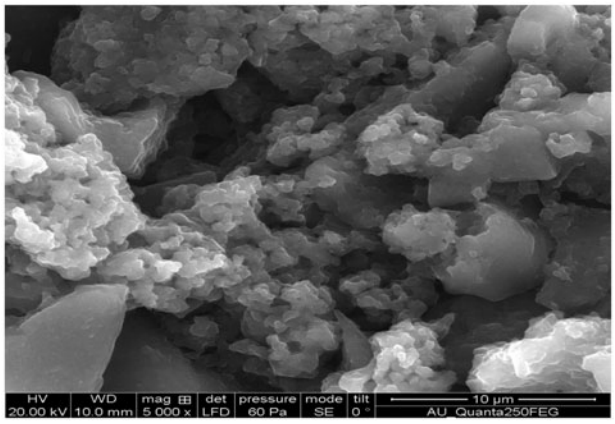

Fig. 3. SEM image of activated DR seed pod.

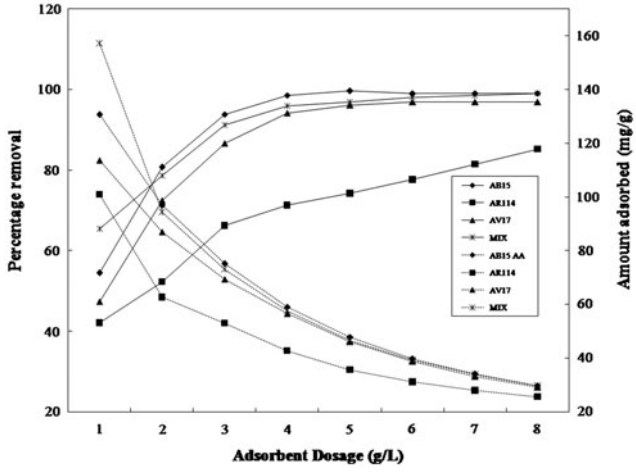

Fig. 4. Effect of adsorbent dosage on the adsorption of AR114, AV17, AB15, and AX onto DR (t = 6 h, C_0 = 120 mg L^{-1}).

3.3. Effect of pH

The pH value of aqueous solution is an important parameter in the adsorption study of anionic dyes because of its effect on both ionization of dye molecules and surface binding sites. All the dyes selected for this study were of anionic in nature, so they release colored dye anions on dissolution. The percentage of color removal decreased when the pH increased from 2 to 11 for all the selected dyes. It may be considered for two possible mechanism of adsorption of dye on the adsorbent: (i) electrostatic interaction between the adsorbent and the dye molecule, (ii) a chemical reaction between the dye and the adsorbent. At pH 2, the concentration of H+ ion increased and the adsorbent surface acquires positive charge by absorbing H+ ions. As the carbon surface is positively

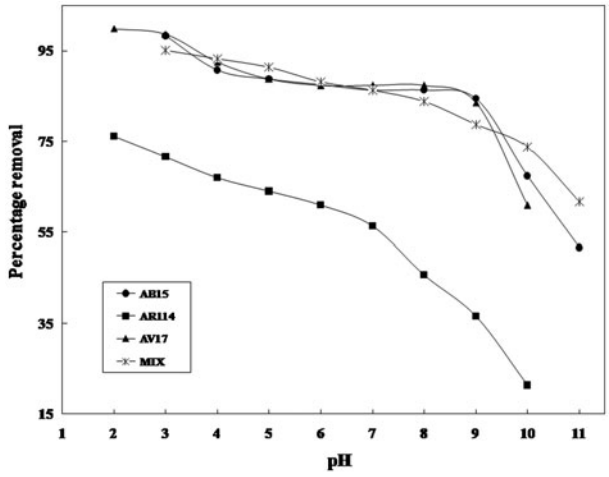

Fig. 5. Effect of pH for the adsorption of AR114, AV17, AB15, and AX onto DR (t = 6 h, C_0 = 100 mg/L, m = 0.1 g/50 mL).

charged at low pH, there may be a high electrostatic attraction exists between the positively charged surface of the adsorbent and the anionic dye molecule, a maximum dye adsorption takes place. The experimental determination of pH_{ZPC} of DR revealed that this activated carbon has pH_{ZPC} 3.9. The initial pH value of the dye solution is 3.2. This mean that the pH of the solution $<pH_{ZPC}$ [15]. Thus, in this case, the activated carbon adsorbent acts as a positive surface and attracts the negatively charged dye molecules. Adsorption of anions is favored at $pH < pH_{zpc}$, while the adsorption of cations is favored at $pH > pH_{zpc}$ [16]. As the pH of the system increases, the number of negatively charged sites increases and the number of positively charged sites decreases. Negatively charged surface sites on the adsorbent surface do not favor the adsorption, due to the electrostatic repulsion. Also lower adsorption of the selected anionic dyes at alkaline pH is due to the presence of excess ^{-}OH ions, which destabilize anionic dyes and compete with the dye anions for the adsorption sites [17]. Adsorption of the selected dyes onto DR as function of pH was examined over a pH range of 2–11 at an initial concentration of C_0 = 100 mg L^{-1}, as shown in Fig. 5. The most effective pH was 2 and it was used in further studies. A similar trend was observed for the adsorption of anionic dyes [17,18].

3.4. Kinetic studies

Contact time is an important factor in the batch adsorption process, because this parameter can affect the adsorption kinetics of an adsorbent for a particular

dye concentration. The kinetic studies for AR114, AV17, AB15, and AX were performed using three different concentrations (60, 80, and 100 mg L^{-1}). The effect of the contact time is that the adsorption efficiency increases rapidly during the initial adsorption stage, and continues to increase at a relatively slow speed with contact time, and reaches equilibrium at 200 min, beyond which constant adsorption was noticed. It was found that the maximum dye adsorption onto the DR was attained in 200 min for all the dyes and its mixture. Adsorption kinetics provides valuable information about the controlling mechanism of the adsorption process. The kinetic data of dye adsorption can be evaluated using four mathematical models.

The pseudo-first-order equation [19] is given by,

$$\log(q_e - q_t) = \log q_e - \frac{k_f t}{2.303} \quad (3)$$

The pseudo-second-order model [20] is given by,

$$\frac{t}{q_t} = \frac{1}{k_s q_e^2} + \frac{1}{q_e} t \quad (4)$$

The Elovich equation [21] is given by,

$$q_t = \frac{1}{\beta} \ln(\alpha\beta) + \frac{1}{\beta} \ln t \quad (5)$$

The linear form of the intraparticle diffusion model [22] is given by,

$$q_t = k_{ip} t^{\frac{1}{2}} + I \quad (6)$$

where q_t is the amount of dye adsorbed on adsorbent at various time t (mg g^{-1}), k_f is the rate constant of pseudo-first-order kinetics (min^{-1}), and t is the contact time (min), k_s is the rate constant of the pseudo-second-order kinetics (g mg^{-1} min^{-1}), α is the initial sorption rate (mg g^{-1} min^{-1}), $1/\beta$ is related to the number of sites available for adsorption (g mg^{-1}), k_{ip} is the intraparticle diffusion rate constant (mg g^{-1} $min^{-½}$), and I is the intercept (mg g^{-1}).

The rate constants, predicted equilibrium uptakes, and their corresponding correlation coefficients for all the dyes studied are summarized in Table 3. The pseudo-first-order kinetics fits well for the first 30 min and thereafter the data deviated greatly from the linearity. Thus, the model represents the initial stages where rapid adsorption occurs, but it cannot be applied for the entire adsorption process [23]. So, the pseudo-first-order model was inapplicable to this system. The correlation coefficients and the $q_{e,cal}$ values from the pseudo-second-order kinetic model are in good agreement with the experimental results. The second-order rate constants of dyes are found to decrease in the following order: AV17 > AB15 > AX > AR114. The values of correlation coefficient of the model were very high and the theoretical q_e values were much closed to the experimental q_e values. The kinetics of adsorption of many dye species onto various adsorbent was also found to be of second-order in literature [3,9,13]. The Elovich equation assumes that the active sites of the adsorbent are heterogeneous and therefore, exhibit different activation energies for chemisorption. When increasing the concentration of dyes, it was observed that the constant α (related to the rate of chemisorption) increased and the constant β (related to the surface coverage) decreased (Table 3), which is due to the decrease in the available adsorption surface for the adsorbates. Therefore, by increasing the concentration, within the range studied, the rate of chemisorption can be increased. The adsorption of acid dyes onto DR follows generally three consecutive steps of external diffusion, intraparticle diffusion, and adsorption. One or more of these steps can control the adsorption kinetics altogether or individually. In a well-agitated batch system, the external diffusion resistance is much reduced. Hence, intraparticle diffusion with the adsorption is more likely to be rate-controlling step [23]. A plot of q_t vs. $t^{1/2}$ should be a straight line (Figure not shown) if intraparticle diffusion is involved in the adsorption process and if these lines pass through the origin, then intraparticle diffusion is the rate-controlling step. In the present study, it was found that the data exhibit multilinear plots then two or more steps influence the sorption process. It is assumed that the external resistance to mass transfer surrounding the particles is significant only in the initial stages of adsorption (initial sharp increase). The second linear portion is the gradual adsorption stage with controlling intraparticle diffusion. When the plots do not pass through the origin, indicates that the pore diffusion is not the sole rate-limiting step but also other kinetic models may control the rate of adsorption, all of which may be operating simultaneously [9]. Therefore, the adsorption kinetics can be satisfactorily approximated by the pseudo-second-order kinetic model, based on the assumption that the rate-limiting step may be chemisorption involving electrostatic forces through the sharing or exchange of electrons between the adsorbent and the adsorbate [13].

Table 3
Kinetic parameters and their correlation coefficients for the adsorption of AR114, AV17, AB15, and AX onto DR

		Pseudo-first-order				Pseudo-second-order			Intraparticle diffusion			Elovich		
Dye	C_0	q_e exp (mg g^{-1})	q_1 (mg g^{-1})	K_1 (min^{-1})	R_1^2	q_2 (mg g^{-1})	$K_2 \times 10^{-3}$ (g mg^{-1} min^{-1})	R_2^2	K_{id} (mg g^{-1} $min^{-½}$)	I	R_I^2	α (mg g^{-1} min^{-1})	β (mg g^{-1})	R_E^2
AR114	60	27.81	22.4957	0.0143	0.9820	31.2500	0.8760	0.9916	1.6712	4.1541	0.9702	16.8305	0.1637	0.9814
	80	43.97	25.2872	0.0113	0.9861	45.2489	1.0934	0.9938	1.9863	14.9125	0.9553	9.9553	0.1361	0.9926
	100	50.51	29.4442	0.0104	0.9755	52.0833	0.9613	0.9920	2.1254	17.8567	0.9160	13.1213	0.1255	0.9753
AV17	60	48.75	23.0834	0.0182	0.9714	52.3560	1.8069	0.9994	1.8583	26.1235	0.8652	43.7393	0.1389	0.9845
	80	44.65	23.7903	0.0150	0.9911	46.7290	1.3920	0.9977	1.8662	18.9732	0.9378	18.3586	0.1433	0.9964
	100	66.54	30.4860	0.0143	0.9892	68.4932	1.1855	0.9981	2.4021	33.2012	0.9352	62.4767	0.1111	0.9952
AB15	60	42.07	22.7500	0.0150	0.9773	44.0529	1.4227	0.9950	1.6302	19.0400	0.9815	28.1245	0.1696	0.9732
	80	35.12	32.7341	0.0129	0.9780	45.8716	0.2879	0.9903	2.5234	21.0680	0.9694	1.5361	0.1098	0.9638
	100	37.83	32.0775	0.0143	0.9815	44.4444	0.5042	0.9978	2.4590	3.5180	0.9573	2.3922	0.1098	0.9937
AX	60	29.48	20.8161	0.0159	0.9844	31.9489	1.2455	0.9888	1.4610	8.7806	0.9732	5.3418	0.1906	0.9518
	80	32.01	17.0294	0.0111	0.9942	32.7869	1.6725	0.9933	1.2910	12.7741	0.9783	13.8606	0.2154	0.9584
	100	35.68	15.1496	0.0122	0.9846	36.3636	2.2335	0.9963	1.1640	18.7923	0.9671	64.4336	0.2348	0.9802

Fig. 6 shows the fitting results using various kinetic models for the adsorbent (DR) for all the dyes studied with an initial concentration of 60 mg L^{-1}. From Fig. 6, pseudo-second-order and Elovich models give comparable fits to the experimental data, while the pseudo-second-order model is better than the Elovich model.

3.5. Adsorption isotherm

Adsorption isotherms parameters from different models provide important information on the surface properties of the adsorbent and its affinity to the adsorbate. Several isotherms models can be used to describe the equilibrium of adsorption. Four common isotherms equations were applied in the present study: Langmuir [24], Freundlich [25], Temkin [26], and Redlich–Peterson [27].

3.5.1. Langmuir isotherm

The Langmuir isotherm model is applied to the equilibrium sorption supposing the monolayer of sorbate on the homogeneous surface with a finite number of identical sites; the linear form the Langmuir model is represented as follows:

$$q_e = \frac{Q_m K_L C_e}{1 + K_L C_e} \text{ or } \frac{C_e}{q_e} = \frac{1}{Q_m K_L} + \frac{C_e}{Q_m} \quad (7)$$

where C_e is equilibrium concentration (mg L^{-1}) of dye, q_e is the amount adsorbed at equilibrium (mg g^{-1}), K_L is the constant related to the free energy of adsorption (L mg^{-1}), and Q_m is the maximum adsorption capacity (mg g^{-1}).

3.5.2. Freundlich isotherm

The Freundlich isotherm is an empirical equation employed to describe heterogeneous systems. The Freundlich equation is commonly given by:

$$q_e = K_F C_e^{\frac{1}{n}} \text{ or } \log q_e = \log K_F + \frac{1}{n} \log C_e \quad (8)$$

where q_e is the amount of solute adsorbed per unit weight of adsorbent (mg g^{-1}), C_e is the equilibrium concentration of the solute in the bulk solution (mg L^{-1}), K_F is a Freundlich constant indicative of the relative adsorption capacity of the adsorbent ($L^{1/n}\, g^{-1}\, mg^{(1-1/n)}$), and $1/n$ is adsorption intensity.

3.5.3. Temkin isotherm

The Temkin isotherm, which considers the effects of the heat of adsorption of all the molecules in the layer decreases linearly with coverage due to adsorbate and adsorbent interactions and the adsorption, is

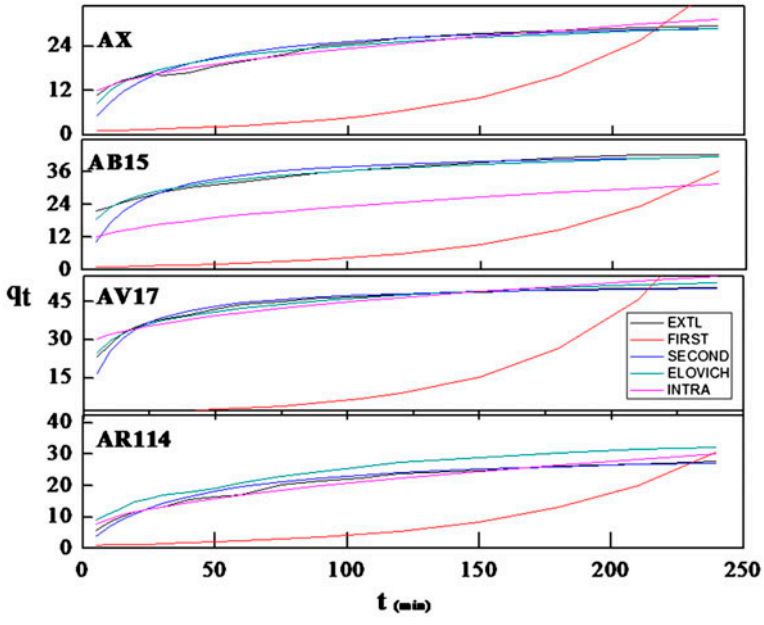

Fig. 6. The fit of experimental adsorption data to Langmuir, Freundlich, and Temkin models for the adsorption AR114, AV17, AB15, and AX onto DR.

characterized by a uniform distribution of binding energies, up to some maximum binding energy. The Temkin isotherm is represented by following equation:

$$q_e = \frac{RT}{b}\ln(K_T C_e) \text{ or } q_e = B_1 \ln K_T + B_1 \ln C_e \quad (9)$$

where $B_1 = RT/b$, K_T is the equilibrium binding constant (L mg^{-1}) and B_1 is the heat of adsorption.

3.5.4. Redlich–Peterson

The Redlich–Peterson isotherm is a combination of Langmuir and Freundlich model. It approaches the Freundlich model at higher concentration and is in accordance with the lower concentration limit of the Langmuir equation. The non-linear Redlich–Peterson isotherm model equation is expressed by:

$$q_e = \frac{K_{RP} C_e}{1 + \alpha_{RP} C_e^{\beta}} \quad (10)$$

where K_{RP} (L g^{-1}) and α_{RP} (L mg^{-1}) are the Redlich–Peterson constants and β is the Redlich–Peterson isotherm exponent, which lies between 0 and 1. The constant β can characterize the isotherm as: if $\beta = 1$, the Langmuir will be the preferable isotherm, while if $\beta = 0$, the Freundlich isotherm will be the preferable isotherm.

The experimental data on the effect of an initial concentration of dyes on the adsorbent DR were fitted to the various isotherm models using MATLAB 7.8.0 (2009a). Fig. 7 shows the comparative fit of Langmuir, Freundlich, Temkin, and Redlich–Peterson isotherms with the equilibrium data plotted as q_e vs. C_e. The isotherm constants for all the isotherms studied and their correlation coefficients with the experimental data are given in Table 4. The correlation coefficient (R^2) for Langmuir isotherm is comparatively higher than those of the Freundlich, Temkin, and Redlich–Peterson isotherms. The Langmuir model presented the high correlation coefficient may giving an indication that chemisorptions (Evidenced by kinetic studies) also be involved in the adsorption process. From the results obtained, it may be observed that the Temkin isotherm does not represent the equilibrium data satisfactorily. Among the dyes studied, adsorption of DR on AR114 showed the highest adsorption capacity (151.5 mg g^{-1}) when compared with other dyes. The adsorbent DR consists of many functional groups to attract the dye molecules on its surface (as also evidenced by the FT-IR spectra Fig. 3). In the adsorption of AR114 onto DR, there may be a high electrostatic attraction between the negatively charged dye molecule (Azo dye Fig. 1) and the positively charged adsorbent surface. This may be

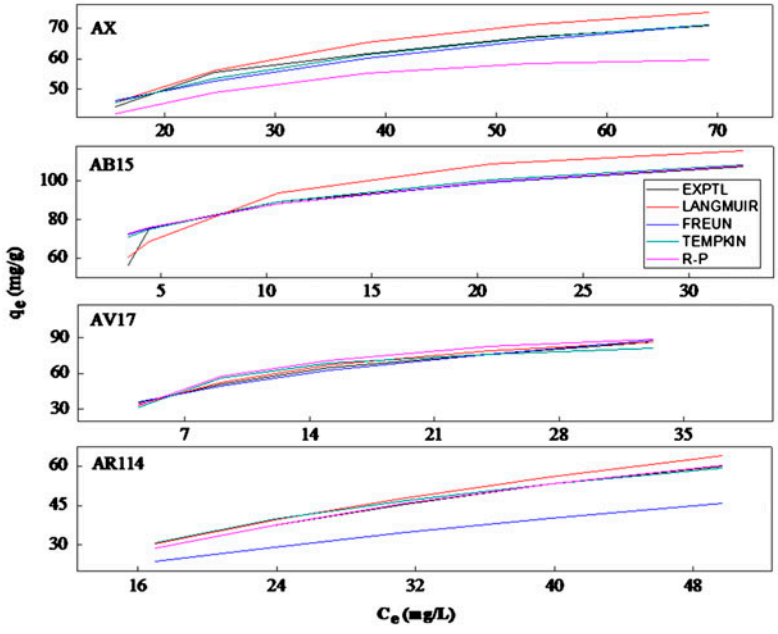

Fig. 7. Comparison between the measured and modeled time profiles for adsorption of AR114, AV17, AB15, and AX onto DR (C_0 = 60 mg/L, m = 0.5 g/L).

Table 4
Langmuir, Freundlich, Temkin, and Redlich–Peterson isotherm model constants for the adsorption of AR114, AV17, AB15, and AX onto DR

Isotherm model	Parameters	AR114	AV17	AB15	AX
Langmuir	q_m	151.51	113.63	129.87	91.87
	K_L	0.0147	0.0957	0.2484	0.0649
	R^2	0.9968	0.9972	0.9972	0.9991
Freundlich	K_F	4.1305	19.0985	57.9429	21.1836
	n	1.4556	2.2936	5.6180	3.4965
	R^2	0.9951	0.9947	0.9971	0.9739
Temkin	K_T	0.0205	0.7812	1.5571	0.9922
	B_1	26.75	25.04	28.33	16.81
	R^2	0.9854	0.9952	0.9904	0.9892
Redlich–Peterson	α	23.64	14.09	58.23	13.58
	β	0.1599	0.0067	0.1767	0.5172
	K_{RP}	2.121	6.316	0.0125	0.894
	R^2	0.8980	0.7452	0.9976	0.9888

due to the presence of two sulfonic acid groups in single phenyl ring, moreover, the activation of DR with 18 N sulfuric acid at a temperature of 120˚C may develops a suitable pore structure, in which the dye molecules are easily accessible. As only pores whose openings are larger than the molecular size of the adsorbate are accessible to the adsorbate. The reduced adsorption capacity of DR with other two dye molecules (AB15AV17) may the adsorbent surface experiences less electrostatic forces of attraction and the adsorbent surface has improper pore size distribution with respect to the dye molecules.

As the mixture of dyes has no particular color hence when compared with the single system. The presence of two or more dyes in solution can and will have an effect on the amount of the dyes adsorbed. The amount of any one dye adsorbed was reduced in the presence of a second dye. Competitive adsorption for active sites on the carbon surface results in a reduction in the overall uptake capacity. The extent of this effect varied with individual dyes and its functional groups [28]. It is evident from the equilibrium studies that equilibrium adsorption capacities decreased in multicomponent systems. The different dye ions will experience different physical and electrical forces according to their structure, molecular size, and functional groups interaction [29]. This may be the possible reason for the low adsorption capacity of the dye mixture AX (91.87 mg g^{-1}). The chemical structures of the dyes (AR114 diazo dye, AB15, and AV 17 are triphenyl methane dyes) and molecular weight could be responsible for the apparent different adsorption capacities. Table 5 shows the comparison of the maximum monolayer adsorption capacities of various adsorbents for dyes. The values of q_m in this study (DR = 151.51 (AR114), 113.63 (AV17), 129.87 (AB15), and 91.87 (AX) mg g^{-1}) are larger than those in most of the previous studies. According to the results obtained, DR could be employed as low-cost adsorbent and could be considered as an alternative to commercial activated carbon for the removal of color.

Table 5
Comparison of adsorption capacities of various adsorbents for acid dyes

Dyes	Adsorbents	q_{MAX} (mg g^{-1})	References
Acid Red 114	Activated *Delonix regia* seed pod	151.51	In this study
Acid Blue 15	Activated *Delonix regia* seed pod	129.87	In this study
Acid Blue 25	Hazelnut shells	60.2	[5]
Methylene blue	Jute fiber	40.58	[6]
Indigo Carmine	Rice husk	29.27	[30]
Acid violet 17	Orange peel	19.88	[18]

4. Conclusion

In this study, the ability of DR to adsorb various acid dyes and its mixture was investigated using kinetic and equilibrium aspects. The adsorption capacity of the dyes on activated carbon increased with decreasing pH. The Langmuir, Freundlich, Temkin, and Redlich–Peterson adsorption models were used to express the sorption phenomenon of acid dyes. The equilibrium data were well described by the Langmuir model. The kinetics of the various dyes adsorbed onto DR was studied using the pseudo-first-order, pseudo-second-order, Elovich, and intraparticle diffusion models. The results indicated that the adsorption kinetics can be satisfactorily approximated by the pseudo-second-order kinetic model, suggesting a chemisorption process. The result of intraparticle diffusion model suggested that it was not the only rate-limiting step. The adsorption capacity of the activated carbon DR in the order AR114 > AB15 > AV17 > AX. This was ascribed to the different chemical natures of the dyes. From these studies, it can be concluded that the activated carbon prepared from DR seed pods is an efficient adsorbent for the color removal of various acid dyes from aqueous solution.

Acknowledgment

The financial support received for the study from the University Grants Commission, New Delhi, India, through major research project (Grant No. F NO 41.266/2012 (SR)) is greatly acknowledged.

References

[1] T. Vernersson, P.R. Bonelli, E.G. Cerrella, A.L. Cukierman, Arundo donax cane as a precursor for activated carbons preparation by phosphoric acid activation, Bioresour. Technol. 83 (2002) 95–104.
[2] G. Crini, Non-conventional low-cost adsorbents for dye removal: A review, Bioresour. Technol. 97 (2006) 61–85.
[3] K. Vasanth Kumar, A. Kumaran, Removal of methylene blue by mango seed kernel powder, Biochem. Eng. J. 27 (2005) 83–93.
[4] L.C. Romero, A. Bonomo, E.E. Gonzo, Acid-activated carbons from peanut shells: Synthesis, characterization and uptake of organic compounds from aqueous solutions, Adsorpt. Sci. Technol. 21(7) (2001) 617–626.
[5] Y. Bulut, Z. Tez, Adsorption studies on ground shells of hazelnut and almond, J. Hazard. Mater. 149 (2007) 35–41.
[6] S. Senthilkumar, P.R. Varadarajan, K. Porkodi, C.V. Subbhuraam, Adsorption of methylene blue onto jute fibre carbon: Kinetics and equilibrium studies, J. Colloid Interface Sci. 284 (2005) 75–82.
[7] M. Auta, B.H. Hameed, Coalesced chitosan activated carbon composite for batch and fixed-bed adsorption of cationic and anionic dyes, Colloids Surf., B 105 (2013) 199–206.
[8] M. Ghaedi, A. Najibi, H. Hossainian, A. Shokrollahi, M. Soylak, Kinetic and equilibrium study of Alizarin Red S removal by activated carbon, Toxicol. Environ. Chem. 94 (2012) 40–48.
[9] Y.S. Ho, R. Malarvizhi, N. Sulochana, Equilibrium isotherm studies of methylene blue adsorption onto activated carbon prepared from *delonix regia* pods, J. Environ. Prot. Sci. 3 (2009) 111–116.
[10] M. Ahmedna, W.E. Marshall, R.M. Rao, Production of granular activated carbons from select agricultural by-products and evaluation of their physical, chemical and adsorption properties, Bioresour. Technol. 71 (2000) 113–123.
[11] P.C.S. Simon, Tables of Spectral Data for Structure Determination of Organic Compounds, second ed., Springer-Verlag, New York, NY, 1983, pp. 63–90.
[12] T. Calvete, E.C. Lima, N.F. Cardoso, J.C.P. Vaghetti, S.L.P. Dias, F.A. Pavan, Application of carbon adsorbents prepared from the Brazilian-pine fruit shell for removal of reactive orange 16 from aqueous solution —Kinetic, equilibrium, and thermodynamic studies, Chem. Eng. J. 91 (2010) 1695–1706.
[13] I.D. Mall, V.C. Srivastava, N.K. Agarwal, I.M. Mishra, Adsorptive removal of malachite green dye from aqueous solution by bagasse fly ash and activated carbon-kinetic study and equilibrium isotherm analyses, Colloids Surf., A 264 (2005) 492–501.
[14] V.K. Garg, M. Amita, R. Kumar, R. Gupta, Basic dye (methylene blue) removal from simulated wastewater by adsorption using Indian Rosewood sawdust: A timber industry waste, Dyes Pigm. 63 (2004) 243–250.
[15] Y.S. Al-Degs, M.I. El-Barghouthi, A.H. El-Sheikh, G.M. Walker, Effect of solution pH, ionic strength, and temperature on adsorption behavior of reactive dyes on activated carbon, Dyes Pigm. 77 (2008) 16–23.
[16] T.L. Seey, M.J.N.M. Kassim, Acidic and basic dyes removal by adsorption on chemically treated mangrove barks, Int. J. Appl. Sci. Technol. 2(3) (2012) 270–276.
[17] P. Senthilkumar, S. Ramalingam, C. Senthamarai, M. Niranjanaa, P. Vijayalakshmi, S. Sivanesan, Adsorption of dye from aqueous solution by cashew nut shell: Studies on equilibrium isotherm, kinetics and thermodynamics of interactions, Desalination 261 (2010) 52–60.
[18] R. Sivaraj, C. Namasivayam, K. Kadirvelu, Orange peel as an adsorbent in the removal of acid violet 17 (acid dye) from aqueous solutions, Waste Manage. 21 (2001) 105–110.
[19] S. Lagergren, Zur theorie der sogenannten adsorption geloster stoffe (About the theory of so-called adsorption of soluble substances), Kungliga Sevenska Vetenskapasakademiens, Handlingar, Band 24(4) (1898) 1–39.
[20] Y.S. Ho, G. Mckay, The kinetics of sorption of basic dyes from aqueous solutions by sphagnum moss peat, Can. J. Chem. Eng. 76 (1998) 822–826.
[21] Y.S. Ho, G. McKay, Comparative sorption kinetic studies of dye and aromatic compounds onto fly ash, J. Environ. Sci. Health. 34(A) (1999) 1179–1204.

[22] W.J. Weber, J.C. Morris, Kinetics of adsorption on carbon solution, J. Sanitary Eng. Division-ASCE. 89 (1963) 31–60.
[23] N. Kannan, M.M. Sundaram, Kinetics and mechanism of removal of Methelene blue by adsorption on various carbons—A comparative study, Dyes Pigm. 51 (2001) 25–40.
[24] I. Langmuir, The adsorption of gases on plane surfaces of glass, mica and platinum, J. Am. Chem. Soc. 40(9) (1918) 1361–1403.
[25] H.M.F. Freundlich, Over the adsorption in solution, J. Phys. Chem. 57 (1906) 385–471.
[26] M.J. Temkin, V. Pyzhev, Kinetics of ammonia synthesis on promoted iron catalysts, Acta Physicochim. URSS. 12 (1940) 217–222.
[27] O. Redlich, D.L. Peterson, A useful adsorption isotherms, J. Phys. Chem. 63 (1959) 1024–1026.
[28] A.A. Attia, E.W. Rashwan, S.A. Khedr, Capacity of activated carbon in the removal of acid dyes subsequent to its thermal treatment, Dyes Pigm. 69 (2006) 128–136.
[29] S.T. Ong, W.N. Lee, P.S. Keng, S.L. Lee, Y.T. Hung, S.T. Ha, Equilibrium studies and kinetics mechanism for the removal of basic and reactive dyes in both single and binary systems using EDTA modified rice husk, Int. J. Phys. Sci. 5(5) (2010) 582–595.
[30] U.R. Lakshmi, V.C. Srivastava, I.D. Mall, D.H. Lataye, Rice husk ash as an effective adsorbent: Evaluation of adsorptive characteristics for Indigo Carmine dye, J. Environ. Manage. 90 (2009) 710–720.